# Metal-Free Visible Light-Mediated Photocatalysis: Controlling Intramolecular [2 + 2] Photocycloaddition of Enones through Axial Chirality

Anthony Clay, Nandini Vallavoju, Retheesh Krishnan, Angel Ugrinov, and Jayaraman Sivaguru*

Department of Chemistry and Biochemistry, North Dakota State University, Fargo, North Dakota 58108, United States

S Supporting Information

ABSTRACT: Atropisomeric enone-imides and enone-amides featuring N-C_{Aryl} bond rotation were evaluated for intramolecular [2 + 2] photocycloaddition. Straight addition product was observed over cross-addition product with good control over reactivity. The atropselectivity was found to be dependent on the substituent on the aryl ring. Substitution-dependent atropselectivity was rationalized on the basis of a divergent mechanistic pathway.
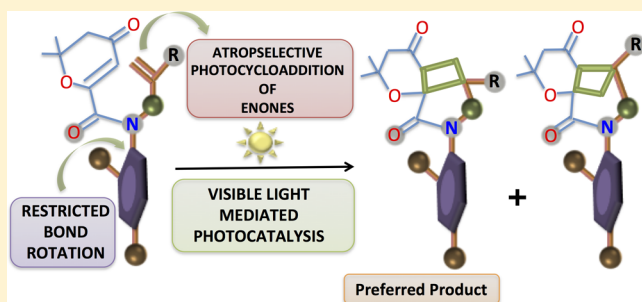
INTRODUCTION

Cyclobutane derivatives are found in numerous naturally occurring compounds with biological activity, ranging from antivirals to antibiotics.[1−7] Consequently, developing new methods for the synthesis of cyclobutanes is of great interest to pharmaceutical, biological, medicinal, and natural product scientists alike. Additionally, cyclobutane analogues have proven to be useful scaffolds for various functional group manipulations in synthetic organic chemistry[1,2,8] and materials chemistry.[9] Photochemistry is unparalleled in its ability to afford complex structural scaffolds from simple and easily accessible reactants. In addition, compounds with multiple stereocenters can be accessed via photochemical processes.[10−12] Often, the short lifetimes involved in photochemical reactions lead to multiple photoproducts with stereocenters limiting their appeal. Efforts to address this complicated reactivity and selectivity in photochemical transformations have met with differing success. Organized media yield among the highest of selectivities due to the lack of degrees of freedom during the photochemical transformation. Supramolecular scaffolds such as crystals, zeolites, molecular cages, and hydrogen bonding templates have been utilized to control excited state reactivity.[13−15] Throughout the past decade, photochemical transformations in the absence of organized media have seen progress with the advent of novel photocatalytic methods. One of the strategies that has received particular attention is photoredox chemistry,[16−23] where a one electron oxidation or reduction of the reactant by a light-absorbing sensitizer generates a ground state radical anion/cation. The increase in the potential of the reactive substrate by electron transfer enhances its reactivity in photoredox chemistry, thereby making it react effectively from the ground state to form pr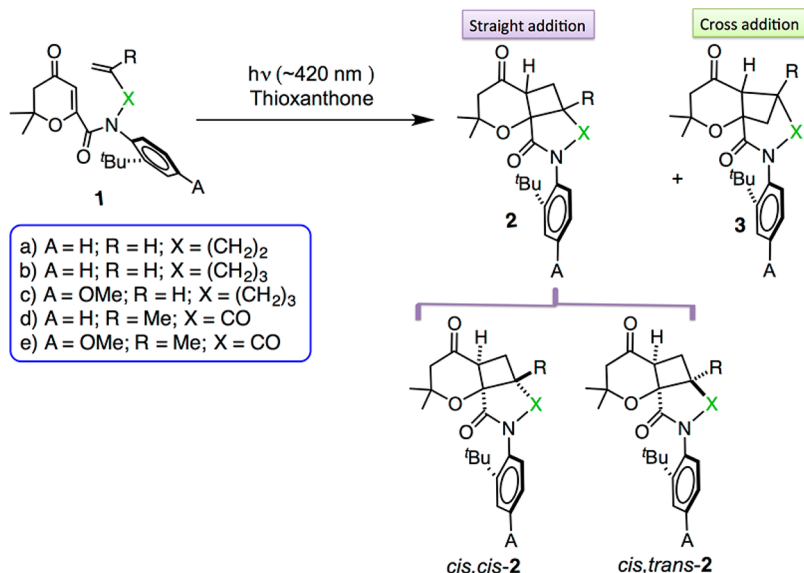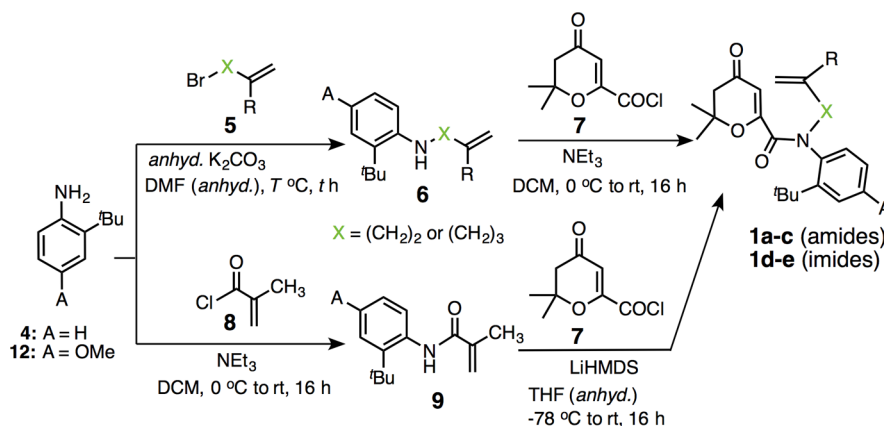oducts. This necessitates evaluation of new approaches to control reactivity and achieve selectivity from the excited state due to its short lifetimes. In this regard, we have employed the use of atropisomeric chromophores[24−32] to control excited state reactivity.[33] We have shown that our strategy[34−44] can be employed to achieve high enantio- and diastereoselectivity in the photoproduct in solution at ambient conditions. The utility of this methodology has been highlighted in various systems with differing photochemical transformations, such as 6π-photocyclization,[34−37] Norrish−Yang cyclization,[38,39] 4π-ring closure,[40] the Paternò−Büchi reaction,[41] and various photocycloadditions.[42−44] In efforts to further increase the scope, display the breadth, and highlight the excited state control of the methodology employed, we focused our attention on [2 + 2] photocycloaddition of enones **1** leading to cyclobutane photoproducts **2/3** (Scheme 1).

Photochemical transformations involving enones have been extensively utilized to synthesize various natural products.[45,46] As enones often feature a mixture of $n\pi^*$ and $\pi\pi^*$ excited states,[47] their reactivities can differ from simple manipulation of reaction conditions. Additionally, the implementation of atropisomers can further alter the reactivity of enones. Various distinguished groups have investigated the intricacies involved in the photochemical cycloadditions of enones.[1,47−50] Piva and co-workers have evaluated the [2 + 2] photocycloaddition of enone-amides with N-allyl substitution where they observed a straight-to-cross addition ratio of 60:40.[51] They also observed that N-substitution impacted both reactivity and selectivity. This allowed us a platform to highlight our methodology involving atropisomers to control the reactivity of enones. In

Scheme 1. Intramolecular Photocycloaddition of Atropisomeric Enones 1

a) A = H; R = H; X = (CH$_2$)$_2$
b) A = H; R = H; X = (CH$_2$)$_3$
c) A = OMe; R = H; X = (CH$_2$)$_3$
d) A = H; R = Me; X = CO
e) A = OMe; R = Me; X = CO

Scheme 2. Synthesis of Atropisomeric Enones 1a−e

this regard, the two sets of enones, enone-amides **1a−c** and enone-imides **1d** and **1e**, were synthesized and their photochemical properties evaluated for atropselective [2 + 2] photocycloaddition.

RESULTS AND DISCUSSION

Atropisomeric enone-amides **1a−c** and enone-imides **1d** and **1e** with varying substitutions were synthesized from the corresponding aniline derivative (Scheme 2) and evaluated for [2 + 2] photocycloaddition.[52] Atropisomeric enones were characterized by ^{1}H and ^{13}C NMR spectroscopy, high-resolution mass spectrometry, and single-crystal XRD.[52] To employ them for controlling photoreactions, we evaluated the activation barrier for racemization (N-C$_{Aryl}$ bond rotation) of enones.[53] The individual atropisomers of enones were separated on a chiral stationary phase using preparative HPLC. As the atropisomers were stable at room temperature, we evaluated the racemization barrier at 45 °C in toluene and acetonitrile. Inspection of Table 1 reveals a high barrier for N−C$_{Aryl}$ bond rotation that was reflected in the high values for $t_{1/2\text{-rac}}$ in both toluene and acetonitrile. Depending on the substitution of the nitrogen (amide vs imide), the racemization

Table 1. Racemization of Atropisomeric Enones[a]

			racemization parameters		
entry	compound	solvent	k_{rac} (days^{-1})	$t_{1/2\text{-rac}}$ (days)	$\Delta G^{\ddagger}_{rac}$ (kcal mol^{-1})
1	**1b**[b]	toluene	1.0	0.7	28.3
2		MeCN	0.7	1.0	28.6
3	**1d**	toluene	1.8	0.4	25.5
4		MeCN	1.4	0.5	25.6
5	**1e**	toluene	1.1	0.6	25.8
6		MeCN	1.1	0.6	25.8

[a]Optically pure isomers were employed for racemization kinetic measurements in a given solvent at a set temperature. Racemization was monitored by HPLC analysis on a chiral stationary phase (error = ± 3%). All measurements were performed at 45 °C unless otherwise indicated. [b]Racemization performed at 75 °C.

barrier was either ∼28 kcal/mol (amides; Table 1, entries 1−2) or ∼26 kcal/mol (imides; Table 1, entries 3−6).

For the reaction conditions (Tables 2 and 3) to be optimized, photoirradiation of enones was carried out under both direct and sensitized irradiations (using visible light with thioxanthone as a triplet sensitizer/catalyst). After the photoreaction, the reaction mixture was concentrated under reduced

Table 2. [2 + 2] Photocycloaddition of Enone-Imide 1d under Direct and Sensitized Irradiations[a]

entry	irradiation conditions	2d (% yield)
1	bb/Pyrex cutoff, 1 h	>98
2	~350 nm, 3 h	>98
3	~420 nm, 9 h	>98
4	420 nm, thioxanthone, 1 h[b]	84

[a]Irradiation of **1d** ($c \approx 2.7$ mM) in MeCN at room temperature under a N_2 atmosphere unless otherwise noted. Values are based on ^{1}H NMR spectroscopy (error = ± 5%). bb/Pyrex cutoff = broadband irradiation performed using a medium pressure 450 W mercury lamp with a Pyrex cutoff (<295 nm cutoff); ~350 nm and ~420 nm irradiations were carried out in a Rayonet reactor. [b]Utilized 10 mol % of thioxanthone.

Table 3. Solvent Effects on [2 + 2] Photocycloaddition Involving Enone-Amide 1b and Enone-Imide 1d with 10 mol % of Thioxanthone[a]

entry	solvent	2b (% yield[b,c])	2d (% yield (dr)[b,d])
1	MCH		>98 (4:1)
2	toluene	15	>98 (3:1)
3	DCM	24	>98 (2:1)
4	chloroform	12	>98 (3:1)
5	EtOAc	18	>98 (2:1)
6	MeOH		>98 (3:1)
7	MeCN	34	84 (4:1)
8	DMSO-d_6		>98 (4:1)

[a]All reactions were performed in a Rayonet reactor at $\lambda \approx 420$ nm using thioxanthone (10 mol %) as a sensitizer; **1b** with 6 h of irradiation), and **1d** with 1 h of irradiation). Values are an average of three runs. [b]The % yield and ratios were determined by ^{1}H NMR spectroscopy using triphenylmethane as an internal standard (error = ± 5%). [c]The ratio of cis,cis-**2b**:cis,trans-**2b** was found to be ~1:1 in all the solvents except EtOAc, where it was 3:2. [d]The **2d** diastereomeric ratio from N-C$_{Aryl}$ bond rotation.

pressure, and the photoproduct(s) was purified by column chromatography and characterized by NMR spectroscopy, HRMS, and single crystal XRD (Table 4). The conversion, yield, and mass balance were calculated by ^{1}H NMR spectroscopy using triphenylmethane as internal standard. Inspection of the crystal structure of the photoproducts shows that, in the case of both enone-amides **1a–c** and enone-imides **1d–e**, the straight addition product **2** was exclusively observed. More importantly, in the case of amides, we observed two stereoisomers, cis,cis-**2** and cis,trans-**2** in approximately 1:1 ratio in the solvents investigated (except for irradiation in EtOAc; Tables 2 and 3). In the cis,cis-**2**, there was cis-fusion of both ring systems (e.g., cis,cis-**1d** features cis-fusion of four-six and four-five ring systems). On the other hand, in cis,trans-**2**, there was cis-fusion of the six-four ring and trans-fusion of the second bicyclic-ring system (e.g., cis,trans-**1d** features cis-fusion of four-six ring system and trans-fusion of four-five ring system). To our surprise, in the case of enone-imides **1d–e**, we observed exclusive formation of cis,cis-**2** as the product.
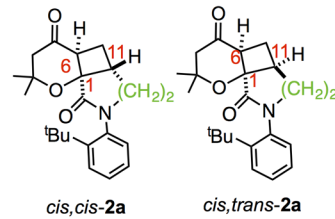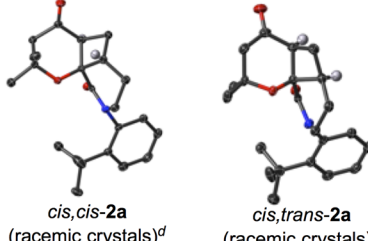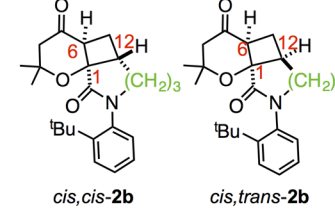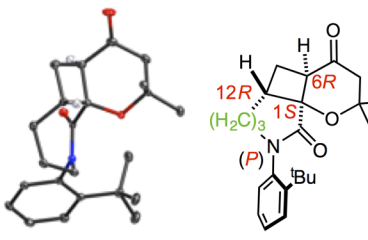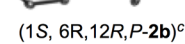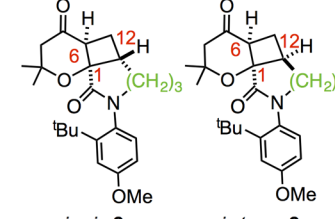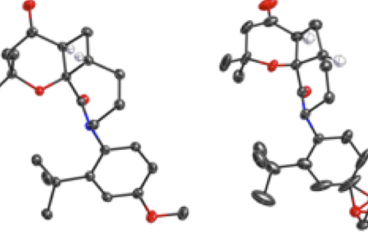
Inspection of Table 2 shows that the reaction of **1d** in acetonitrile was efficient both under direct irradiation (Pyrex cutoff) and visible light irradiation with 10 mol % loading of thioxanthone (acting as a catalyst/sensitizer). Inspection of Table 3 shows that the [2 + 2] photocycloaddition of enone-imide **1d** was clean and efficient when compared to the enone-

amide **1b**. Enone-imide **1d** gave excellent yield and mass balance in all of the investigated solvent systems. For the efficiency of the reaction with enone-amide **1b** in different solvents to be compared, the irradiation time was kept constant at 6 h with the conversion varying from 12 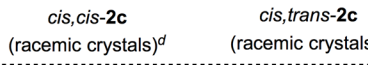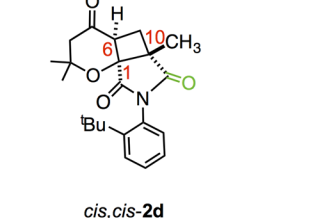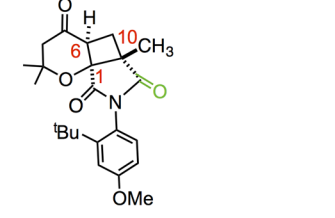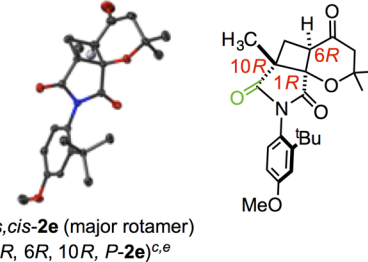to 34% (Table 2). Higher irradiation time gave higher conversions. Alternatively, excellent yield was observed with enone-amides **1b** and **1c** upon direct irradiation at ~350 nm (Table 4, entries 2 and 5). It can be inferred from examination of Tables 3 and 4 that the type of functionality and the length of the N-alkenyl chain of atropisomeric enones played a crucial role in determining the product distribution. With respect to enone-imides **1d** and **1e**, we observed exclusive formation of the corresponding cis,cis-**2** as the product. As we had employed a racemic mixture of atropisomeric reactant **1d** and **1e**, we observed two diastereomeric rotamers of cis,cis-**2d**, which arise due to rotation of the N–C$_{Aryl}$ bond (Table 4, entries 8 and 9). More importantly, we were able to separate the diastereomeric rotamers by chromatography and confirmed their relationship by ^{1}H NMR spectroscopy and by single crystal XRD analysis.[52] Both the major and minor diastereomeric rotamers of cis,cis-**2d** crystallized as racemic crystals (containing a mixture of enantiomers; Table 4, entry 8). From single crystal XRD analysis, the configuration of the minor diastereomeric rotamer of cis,cis-**2d** was established as (1R,6R,10R,M)-**2d** and (1S,6S,10S,P)-**2d**. Similarly, from single crystal XRD analysis, the configuration of the major diastereomeric rotamer of cis,cis-**2d** was established as (1R,6R,10R,P)-**2d** and (1S,6S,10S,M)-**2d**. To our surprise, we were able to isolate the chiral crystal of the major diastereomeric rotamer of cis,cis-**2e** (as it was a mixture of conglomerate crystals of individual enantiomers) and established its absolute configuration as (1R,6R,10R,P)-**2e** (Table 4, entry 9). The major and minor rotamers in cis,cis-**2d** differed only by rotation about the N-C$_{Aryl}$ bond (the same is true for cis,cis-**2e**).[29,31,53−56] Heating of the minor diastereomeric rotamer of cis,cis-**2d** in DMSO-d_6 resulted in the major diastereomeric rotamer cis,cis-**2d** (Scheme 3).[52] The rate constant (monitored by NMR spectroscopy) for N-C$_{Aryl}$ bond rotation was found to be 1.7×10^{-7} s^{-1} at 75 °C in DMSO-d_6.

To evaluate the role of axial chirality in determining the stereochemistry of the product, we carried out the photochemical reaction of optically pure atropisomers of amides **1b** and **1c**. High enantioselectivity was observed in the photoproduct during the photochemical transformation of optically pure atropisomers of enone-amide **1b**.[57] To our surprise, para-methoxy derivative **1c** gave near racemic photoproducts cis,cis-**2c** and cis,trans-**2c**. This necessitated a mechanistic understanding to rationalize the behavior of enones (vide infra).

In an effort to understand the mechanistic details, photophysical measurements were obtained for **1d**. At 77 K, there was no observable phosphorescence, showing that there is efficient deactivation of the excited state by another pathway. As the reaction was efficient with thioxanthone (TX) acting as a visible light photocatalyst/sensitizer, we investigated its role in promoting the reaction using transient absorption studies. Laser excitation (λ_{ex} = 355 nm; 7 ns pulse width; 5 mJ/pulse) of TX in the presence of varying concentrations of **1d** in N_2-degassed acetonitrile solution showed that the triplet of thioxanthone was efficiently quenched (Figure 1) with a bimolecular quenching rate constant (k_q) 8.2×10^9 M^{-1} s^{-1}.[44,58] No new transient species were observed, and the bleach at 380 nm showed very fast recovery in the presence of **1d**. The

Table 4. Intramolecular [2 + 2] Photocycloaddition of Atropisomeric Enones[a]

Entry	Substrate	t (h)	Photoproduct	% yield / selectivity	Single crystal XRD	
1	1a	12	cis,cis-2a cis,trans-2a	Yield = 88% 2a : 3a = >49 : 1 cis,cis-2a: cis,trans-2a = 3:1	cis,cis-2a (racemic crystals)[d]	cis,trans-2a (racemic crystals)[d]
2	1b	7	cis,cis-2b cis,trans-2b	Yield = 73% (isolated yield)[b] 2b : 3b = >49 : 1 cis,cis-2b: cis,trans-2b = 1:1	(1S, 6R,12R,P-2b)[c]	
3	pkA-1b			cis,cis-2b: 91% ee		
4	pkB-1b			ent-cis,cis-2b: 86% ee		
5	1c	6	cis,cis-2c cis,trans-2c	Yield = 66% (isolated yield)[b] 2c : 3c = >49 : 1 cis,cis-2c: cis,trans-2c = 1:1	cis,cis-2c (racemic crystals)[d]	cis,trans-2c (racemic crystals)[d]
6	pkA-1c			cis,cis-2c: <5% ee		
7	pkB-1c			ent-cis,cis-2c: <5% ee		
8	1d	1	cis,cis-2d	cis,cis-2d: cis,trans-2d = >49:1 Yield = 84% 2d : 3d = >49 : 1 N-C_Aryl rotamer ratio cis,cis-2d = 4 : 1	cis,cis-2d (major rotamer) (racemic crystals)[d] (1R, 6R, 10R, P-2d) and (1S, 6S, 10S, M-2d)	cis,cis-2d (minor rotamer) (racemic crystals)[d] (1R, 6R, 10R, M-2d) and (1S, 6S, 10S, P-2d)
9	1e	1	cis,cis-2e	cis,cis-2e: cis,trans-2e = >49:1 Yield = 99% (70% isolated) 2e : 3e = >49 : 1 N-C_Aryl rotamer ratio cis,cis-2e = 4: 1	cis,cis-2e (major rotamer) (1R, 6R, 10R, P-2e)[c,e]	

[a]Irradiations were carried out with 10 mol % of thioxanthone in a Rayonet reactor equipped with ~420 nm (16 bulbs ×14 W) unless otherwise noted. Reaction carried out with the 1:1 mixture of atropisomers. For atropselective reaction in entries 3, 4, 6, and 7, optically pure atropisomers that were separated from HPLC were employed. pkA and pkB refer to the first and second peak that elutes out of the HPLC on a chiral stationary phase. Reported values carry an error of ±5%. [b]Isolated yields for **1b** and **1c** were determined from direct irradiation conditions in a Rayonet reactor at ~350 nm (16 bulbs ×14 W). Visible light irradiation was also effective and gave similar selectivity. [c]Stereochemistry was deduced from single crystal XRD analysis using Flack parameters. [d]Racemic crystals of **2d** (major and minor rotamers of cis,cis-**2d**) had both of the enantiomeric forms within the same unit cell. [e]Optically pure crystals from **2e** were picked from a mixture of conglomerate crystals.
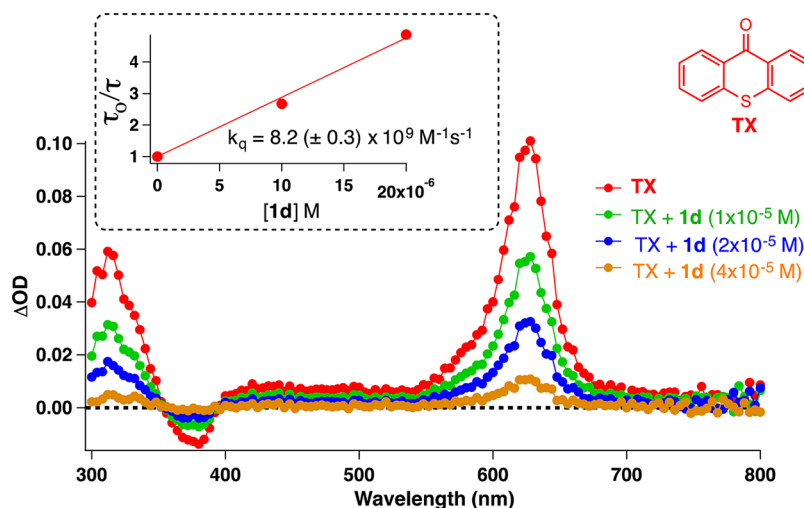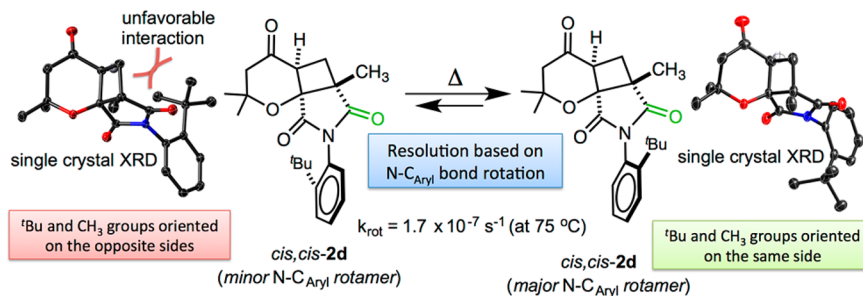
Scheme 3. N-C$_{Aryl}$ Bond Rotation in *cis,cis*-2d

Figure 1. Quenching studies of thioxanthone (TX) in the presence of **1d**. Laser flash photolysis performed using Nd:YAG laser (355 nm, 5 mJ/pulse, 7 ns pulse width). The transient absorption spectra were plotted 4 μs after laser flash. (Inset) Stern–Volmer quenching plot of TX in the presence of **1d**.

photophysical data implicates an energy transfer pathway rather than electron transfer from the excited thioxanthone to the enone.

On the basis of the above results, we postulate that the enone reaches the triplet excited state upon energy transfer from excited thioxanthone. On the basis of the triplet state reactivity of enone with electron-deficient alkene (as in the case of imides **1d** and **1e**), the reaction is likely triggered by a $\pi^* \to \pi^*$ interaction[47] between the excited enone and the electron deficient alkene leading to biradical **BR2** that cyclizes to form *cis,cis*-**2** products. Upon increasing the chain length of the *N*-alkenyl substituent (as in amide **1a** or **1b**), the longer flexible alkenyl chain likely orients itself by exposing one of the two faces of the alkene double-bond to the excited enone leading to **BR2**, which cyclizes to *cis,cis*-**2** and *cis,trans*-**2** products.[44] In a parallel scenario, our present mechanism cannot rule out the formation of **BR3** in the reaction pathway as it can lead to *cis,cis*-**2** and *cis,trans*-**2** products. However, considering that the reaction is likely originating from the π^* of excited enone, this intermediate is less likely. The last aspect we will address is the loss of atropselectivity with enone-amide **1c** that features a *para*-methoxy substituent. The electron transfer pathway has previously been implicated for hydrogen abstraction involving amido-cycloalkenones.[59] On the basis of this precedence, we believe the electron-rich nature of the *p*-OMe substituent likely triggers an electron transfer pathway leading to loss of axial chirality. This results in the loss of atropselectivity (Scheme 4), which is reflected in the near racemic product despite

employing optically pure atropisomers in **1c** (Table 4, entries 6 and 7).

■ CONCLUSIONS

Our study has showcased that intramolecular [2 + 2] photocycloaddition of excited enone could be effectively controlled by incorporating axial chirality into the system. The selectivity is dependent on the type of substituent on the nitrogen. For short chain imide substituents, exclusive formation of straight addition was observed. Our results showcase that one may achieve excellent control of excited-state reactivity by employing restricted bond rotation(s) leading to stereoenriched product(s). Controlling such transformations under visible light-mediated photocatalytic conditions will open avenues to devise strategies to perform light-initiated reactions in a stereocontrolled fashion.[60−62]

■ EXPERIMENTAL SECTION

General Methods. All commercially obtained reagents/solvents were used as received without further purification. Spectrophotometric grade solvents (ethanol and methylcyclohexane) were purchased and used without further purification for emission measurements. Unless stated otherwise, reactions were conducted in oven-dried glassware under nitrogen atmosphere. ^{1}H and ^{13}C NMR spectra were recorded on 400 MHz (100 MHz for ^{13}C) and on 500 MHz (125 MHz for ^{13}C) spectrometers. Data from the ^{1}H NMR spectroscopy are reported as chemical shifts (δ ppm) with the corresponding integration values. Coupling constants (J) are reported in hertz (Hz). Standard abbreviations indicating multiplicity were used as follows: s (singlet), b (broad), d (doublet), t (triplet), q (quartet), m (multiplet), and virt

Scheme 4. Mechanistic Aspects of [2 + 2] Photocycloaddition in Atropisomeric Enones
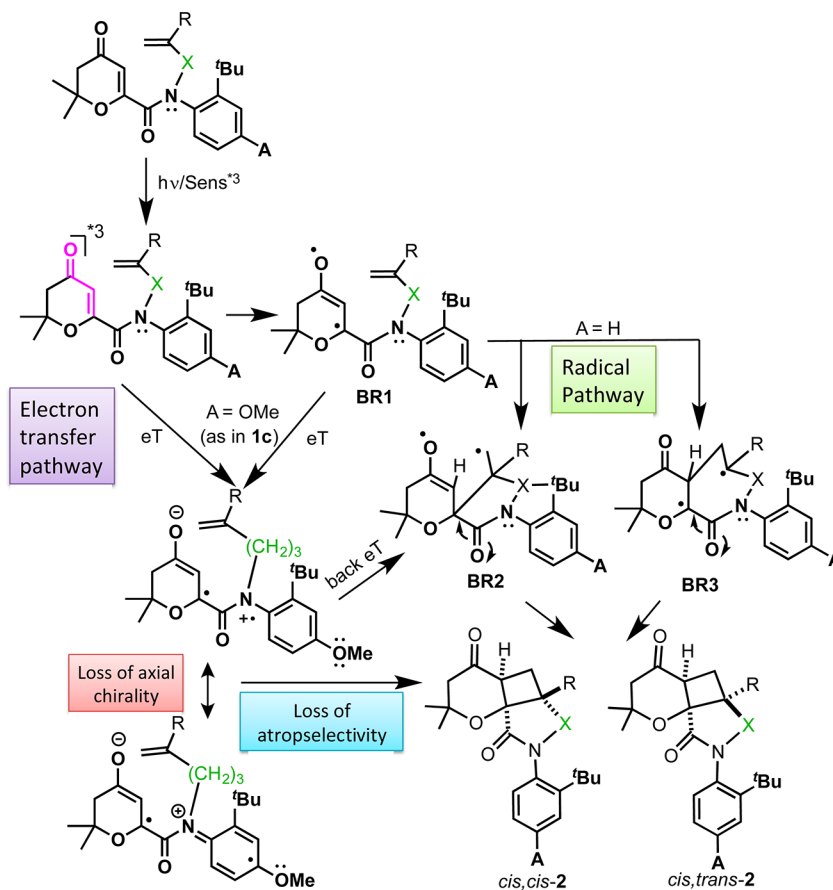
(virtual). Data for ^{13}C NMR spectra are reported in terms of chemical shift (δ ppm). In many instances it was not possible to obtain the signal for the carbonyl carbon, wherever possible we have reported all of the signals. High-resolution mass spectrum data in electrospray ionization mode were recorded in positive (ESI$^+$) ion mode. HPLC analyses were performed on analytical HPLC. Preparative HPLC was used for automated sample injection and separation of atropisomers. All HPLC injections were monitored using a dual wavelength absorbance detector at 254 and 270 nm or using a diode array detector. Analytical and semipreparative injections were performed on the chiral stationary phase using various columns as indicated below. (R,R) WHELK-01; 25 cm × 4.6 mm column for analytical injections; 25 cm × 10 mm column for semipreparative injections. CHIRAPAK AD-H; 0.46 cm × 25 cm column for analytical injections; 10 mm × 25 cm column for semipreparative injections. UV–vis spectra were recorded using UV quality fluorimeter cells (with range until 190 nm). When necessary, the compounds were purified by column chromatography using hexanes:ethyl acetate as the mobile phase silica as stationary phase.

Photophysical Methods. Spectrophotometric solvents were used when necessary unless otherwise mentioned. UV quality fluorimeter cells (with range until 190 nm) were used for optical measurements. Emission spectra were recorded on a spectrometer equipped with double-grating monochromators, dual lamp housing containing a 450-W CW xenon lamp and a xenon flash lamp, Fluorohub/MCA/MCS electronics, and a PMT detector. The nanosecond transient absorption experiments were performed with a laser flash photolysis kinetic spectrometer equipped with a 300 mm focal length monochromator in Czerny Turner configuration and an analyzing photomultiplier featuring a side window photomultiplier detector. The pulses for the experiment were from a third harmonic ultra compact flash lamp pumped Nd:YAG laser (355 nm, 5 mj/pulse, 7 ns pulse width).

X-Ray Crystal Structure Determination. Single crystal X-ray diffraction data of the compounds **2a–e** were collected on an XRD diffractometer equipped with a CCD area detector at T = 100 K. Cu radiation was used. A direct method was used to solve the structures after multiscan absorption corrections. Details of data collection and refinement are given in the Supporting Information. All thermal ellipsoid plots were generated with 50% probability.

Synthesis of 4-Amino-3-tert-butylphenol 11. Following a reported procedure,[63] a solution of sulfanilic acid **10** (55.9 mmol, 1.2 equiv) and Na$_2$CO$_3$ (28 mmol, 0.6 equiv) was prepared in 60 mL of deionized H$_2$O and set to reflux for 30 min. The solution became colorless yet turbid until it began to reflux, where it turned pale yellow and turbid and then became clear. After reflux, the clear pale yellow solution was cooled to 0 °C. Then, NaNO$_2$ (55.9 mmol, 1.2 equiv) was dissolved in 25 mL and added dropwise to the reaction mixture. The reaction mixture became dark yellow. The yellow solution was added to a mixture of 9 mL of concentrated HCl and 56 g of ice. The resulting yellow solution was added to another solution containing 3-tert-butylphenol **15** (46.6 mmol, 1 equiv) prepared in 20% NaOH (note, both solutions were cooled to 0 °C.). The blood red solution was allowed to stir at room temperature overnight. Approximately 16 h later, the red mixture was allowed to stir at 60 °C, and Na$_2$S$_2$O$_4$ (140 mmol, 3 equiv) was added portion-wise. Upon addition of Na$_2$S$_2$O$_4$, the solution became brownish yellow in color. After 30 min, the reaction mixture was cooled to room temperature and filtered. The filter cake was extracted with CHCl$_3$ (3 × 30 mL) and refiltered after every extraction. The organic portions were combined, washed with 5% Na$_2$CO$_3$ solution and then brine, dried, and concentrated. The dark purple solid was confirmed to be the product by ^{1}H NMR spectroscopy. Compound **11** was used without further purification in the subsequent step as a dark purple solid (68% yield, 1.5 g); ^{1}H NMR (400 MHz, CDCl$_3$) δ 6.75 (t, J = 1.6 Hz, 1H), 6.52 (d, J = 1.6 Hz, 2H), 4.27 (bs, 1H), 3.54 (bs, 2H), 1.38 (s, 9H).

Synthesis of 4-Amino-3-tert-butylanisole 12. Following a reported procedure,[63] compound **11** (18.6 mmol, 1 equiv) and KO^tBu (19 mmol, 1.02 equiv) were evacuated and purged with N_2 and then dissolved in DMSO (10 mL). The reaction mixture was allowed to stir for 1 h before the addition of Me_2SO_4 (19.7 mmol, 1.06 equiv). After 15 min, the reaction was quenched with water, extracted with Et_2O, washed with brine, dried over Na_2SO_4, filtered, and concentrated. The organic layer was dried over anhyd Na_2SO_4 and filtered, and the solvent was removed under reduced pressure to obtain the crude product. The crude reaction mixture was purified via Combiflash using 80:20 hexanes:EtOAc as the mobile phase. Aniline derivative **12** was a brown oil (40% yield, 0.66 g); ^{1}H NMR (400 MHz, CDCl3) δ 6.85 (m, 1H), 6.60 (m, 2H), 3.73 (s, 3H), 3.55 (bs, 2H), 1.40 (s, 9H); ^{13}C NMR (100 MHz, CDCl3) δ 152.9, 138.5, 136.1, 119.0, 111.3, 55.8, 34.7, 29.8.

Synthesis of Ethyl 2,2-Dimethyl-4-oxo-3,4-dihydro-2H-pyran-6-carboxylate 13. Enone **13** derivative was synthesized according to a procedure reported in the literature.[64] A flask was evacuated and purged with N_2. Absolute ethanol (EtOH) was added to the empty round-bottom flask under nitrogen. Then, mixtures of mesityl oxide **16** (10.2 mmol, 1 equiv) and diethyl oxalate **17** (10.2 mmol, 1 equiv) in EtOH were added to the round-bottom flask at 0 °C. After the reaction mixture was allowed to stir for 5 min, sodium ethoxide in ethanol (21 wt%; ~11.2 mmol, ~1.1 equiv) was added dropwise over 20 min. The resulting reaction mixture was dark yellow in color. The reaction mixture was allowed to stir at 0 °C for an additional 10 min before slowly rising to room temperature. The reaction mixture was allowed to stir overnight. After approximately 20 h, the reaction was diluted with diethyl ether and then poured into a flask containing 2 N H_2SO_4 (~5 mL concd acid into 76 mL of H_2O). The organic layer was separated, and the aqueous layer was extracted with ethyl acetate. The crude product was purified by Combiflash yielding a light yellow oil (60% yield, 2.4 g); ^{1}H NMR (400 MHz, CHCl3) δ 6.18 (s, 1H), 4.30 (q, J = 7.1 Hz, 2H), 2.52 (s, 2H), 1.47 (s, 6H), 1.33 (t, J = 7.1 Hz, 3H); ^{13}C NMR (100 MHz, CDCl3) δ 193.8, 162.3, 157.4, 107.5, 82.7, 62.6, 47.8, 26.0, 14.2.

Synthesis of 3,4-Dihydro-2-,2-dimethyl-4-oxo-2H-pyran-6-carboxylic Acid 14. To a solution of **13** (2 g) in THF (45 mL) was added 5 M HCl (30 mL), which was stirred for 24 h or until precipitation occurred. After starting material was consumed, the solvent was removed under vacuum, followed by washing with water and removing solvent under vacuum. The crude product was purified by recrystallization in a THF:hexanes mixture to yield an off white solid (80% yield, 1.7 g); ^{1}H NMR (400 MHz, CDCl3) δ 6.30, (s, 1H), 2.57 (s, 2H), 1.50 (s, 6H).

Synthesis Protocol for N-Substituted Anilines 6a–c. Following a reported procedure,[44] the appropriate aniline derivative (**4** or **12**) (6.7 mmol, 1.5 equiv) was added to activated K_2CO_3 (11.2 mmol, 2.5 equiv) in a round-bottom flask and combined with a stir bar, then evacuated and purged with N_2. The mixture was then dissolved in DMF (22 mL) followed by the addition of bromoalkene **5a** or **5b** (4.5 mmol, 1 equiv). The reaction mixture was set to 90 °C and allowed to stir overnight. After ~16 h, the reaction mixture was removed from heat, quenched with H_2O, and then extracted with EtOAc followed by washing with brine solution. The organic layers were combined, dried over Na_2SO_4 (anhyd), filtered, concentrated, and purified by combiflash hexanes:EtOAc (95:5) as the mobile phase.

Compound **6a**: yellow liquid (44% yield, 1.5 g); ^{1}H NMR (400 MHz, CDCl3) δ 7.23–7.20 (m, 1H), 7.12–7.08 (m, 1H), 6.68–6.64 (m, 2H), 5.89–5.79 (m, 1H), 5.21–5.12 (m, 3H), 3.96 (bs, 1H), 3.22 (t, J = 6.4 Hz, 3H), 2.48–2.43 (m, J = 3H), 1.37 (s, 9H); ^{13}C NMR (100 MHz, CDCl3) δ 146.6, 136.6, 133.3, 127.3, 126.4, 117.6, 117.0, 111.7, 43.4, 34.0, 30.1; HRMS (ESI/TOF-Q) m/z calcd for $C_{14}H_{21}NH^+$ [M + H]^+ 204.1752, found 204.1760.

Compound **6b**: amber liquid (76% yield, 0.55 g); ^{1}H NMR (400 MHz, CDCl3) δ 7.23 (m, 1H), 7.16–7.12 (m, 1H), 6.69 (t, J = 7.4 Hz, 2H), 5.94–5.82 (m, 1H), 5.13–4.99 (m, 2H), 3.86 (s, 1H), 3.21 (t, J = 7.0 Hz, 2H), 2.27–2.19 (m, 2H), 1.85–1.77 (m, 2H), 1.43 (s, 9H); ^{13}C NMR (100 MHz, CDCl3) δ 146.7, 138.2, 133.2, 127.4, 126.4,

117.0, 115.4, 111.8, 44.0, 34.4, 31.8, 30.2, 29.1; HRMS (ESI/TOF-Q) m/z calcd for $C_{15}H_{23}NH^+$ [M + H]^+ 218.1909, found 218.1918.

Compound **6c**: amber liquid (66% yield, 0.61 g); ^{1}H NMR (400 MHz, CDCl3) δ 6.89–6.88 (m, 1H), 6.71–6.68 (m, 1H), 6.63–6.61 (m, 1H), 5.91–5.80 (m, 1H), 5.09–4.97 (m, 2H), 3.74 (s, 3H), 3.56 (bs, 1H), 3.13 (t, J = 7.0 Hz, 2H), 2.24–2.16 (m, 2H), 1.82–1.73 (m, 2H), 1.40 (s, 9H); ^{13}C NMR (100 MHz, CDCl3) δ 151.8, 141.1, 138.3, 135.8, 115.3, 114.5, 113.2, 110.8, 55.9, 45.0, 34.6, 31.8, 30.1, 29.2; HRMS (ESI/TOF-Q) m/z calcd for $C_{16}H_{25}NOH^+$ [M + H]^+ 248.2014, found 248.2021.

Synthesis of Amides 9a and 9b. A literature procedure[43] was employed as reported for the synthesis of amides **9a** and **9b**. To a solution of the aniline derivative **4** or **12** (1.0 g, 1.0 equiv), and triethylamine (2.0 equiv) in dry DCM (15 mL) at 0 °C under a N_2 atmosphere was added the corresponding acyl chloride **8** (1.1 equiv). The resulting solution was slowly allowed to warm to room temperature over 16 h. After the reaction, water was added and stirred, and the layers were separated. The organic layer was washed with DI water (2 × 15 mL), dried over anhyd Na_2SO_4 and filtered, and the solvent was removed under reduced pressure to yield the crude product. The crude product was purified by combiflash using hexanes:ethyl acetate as the mobile phase.

Compound **9a**: colorless solid (80% yield, 2.91 g); mp 104–107 °C; ^{1}H NMR (400 MHz, CDCl3) δ 7.66–7.64 (m, 1H), 7.59 (bs, 1H), 7.39–7.37 (m, 1H), 7.23–7.19 (m, 1H), 7.16–7.13 (m, 1H), 5.82 (s, 1H), 5.45 (d, J = 0.6 Hz, 1H), 2.07 (s, 3H), 1.40 (s, 9H); ^{13}C NMR (100 MHz, CDCl3) δ 166.6, 142.4, 141.2, 135.4, 127.7, 127.0, 126.7, 126.2, 120.0, 34.7, 30.9, 19.1; HRMS (ESI/TOF-Q) m/z calcd for $C_{14}H_{19}NOH^+$ [M + H]^+ 218.1545, found 218.1545.

Compound **9b**: pale yellow solid (50% yield, 0.520 g); mp 127–129 °C; ^{1}H NMR (400 MHz, CDCl3) δ 7.43–7.36 (m, 1H), 6.94–6.93 (m, 1H), 6.76–6.73 (m, 1H), 5.81 (s, 1H), 5.43 (s, 1H), 3.78 (s, 3H), 2.05 (s, 3H), 1.37 (d, J = 2.2 Hz, 9H); ^{13}C NMR (100 MHz, CDCl3) δ 167.0, 157.9, 145.5, 141.0, 130.0, 128.1, 119.9, 113.9, 110.7, 55.6, 35.0, 30.7, 19.1; HRMS (ESI/TOF-Q) m/z calcd for $C_{15}H_{21}NO_2Na^+$ [M + Na]^+ 270.1470, found 270.1478.

Synthesis of Substituted Atropisomeric Enone-Amides 1a–c. To a solution of N-alkenyl aniline derivative **6a**, **6b**, or **6c** (1.0 g, 1.0 equiv), triethylamine (2.0 equiv) in dry DCM (15 mL) at 0 °C under N_2 atmosphere the corresponding acyl chloride **7** (1.1 equiv) was added. The resulting solution was slowly allowed to warm to room temperature and stir for 16 h. After the reaction, water was added, stirred and the layers were separated. The organic layer was washed with DM water (2 × 15 mL), dried over *anhyd.* Na_2SO_4, filtered and the solvent was removed under reduced pressure to yield crude product. The crude product was purified by combiflash using hexanes:ethyl acetate mixture.

Compound **1a**: yellow liquid (70% yield, 1.82 g); ^{1}H NMR (400 MHz, CDCl3) δ 7.48 (dd, J = 8.1, 1.3 Hz, 1H), 7.27–7.19 (m, 1H), 7.08–7.01 (m, 1H), 6.87 (dd, J = 7.8, 1.4 Hz, 1H), 5.75–5.60 (m, 2H), 5.04–4.92 (m, 2H), 4.33 (ddd, J = 12.9, 10.0, 6.1 Hz, 1H), 2.91–2.75 (m, 1H), 2.48–2.36 (m, 1H), 2.27–2.07 (m, 3H), 1.32 (d, J = 1.2 Hz, 9H), 1.00 (s, 3H), 0.69 (s, 3H); ^{13}C NMR (100 MHz, CDCl3) δ 192.5, 164.1, 162.9, 146.8, 138.3, 134.93, 132.1, 130.6, 128.8, 126.3, 117.2, 105.9, 82.6, 51.6, 47.4, 36.5, 32.6, 30.9, 26.3, 24.3; HRMS (ESI/TOF-Q) m/z calcd for $C_{22}H_{29}NO_3H^+$ [M + H]^+ 356.2243, found 356.2226.

Compound **1b**: opaque white solid (77% yield, 0.65 g); mp 55–59 °C; ^{1}H NMR (400 MHz, CDCl3) δ 7.55–7.52 (m, 1H), 7.31–7.27 (m, 1H), 6.91–6.89 (m, 1H), 5.77–5.70 (m, 2H), 4.99–4.94 (m, 2H), 4.32–4.25 (m, 1H), 2.88–2.81 (m, 1H), 2.34–2.14 (m, 2H), 2.07–1.86 (m, 4H), 1.61–1.54 (m, 1H), 1.38 (s, 9H), 1.05 (s, 3H), 0.75 (s, 3H); ^{13}C NMR (100 MHz, CDCl3) δ 192.7, 164.2, 162.8, 146.7, 138.5, 137.6, 132.0, 130.6, 128.8, 126.3, 115.5, 105.9, 82.6, 52.2, 47.5, 36.6, 32.6, 31.3, 26.4, 25.4, 24.4; HRMS (ESI/TOF-Q) m/z calcd for $C_{23}H_{31}NO_3H^+$ [M + H]^+ 370.2385, found 370.2382.

Compound **1c**: pale yellow solid (49% yield, 0.48 g); mp 84–86 °C; ^{1}H NMR (400 MHz, CDCl3) δ 7.03–7.02 (m, 1H), 6.83–6.80 (m, 1H), 6.63–6.61 (m, 1H), 5.78–5.68 (m, 2H), 4.99–4.91 (m, 2H), 4.29–4.22 (m, 1H), 3.77 (s, 3H), 2.84–2.77 (m, 1H), 2.35–2.15

(ABq, J = 16.4 Hz, 2H), 2.10–2.05 (m), 1.99–1.88 (m, 1H), 1.83–1.79 (m, 1H), 1.63–1.61 (m, 1H), 1.36 (s, 9H), 1.10 (s, 3H), 0.82 (s, 3H); ^{13}C NMR (100 MHz, CDCl$_3$) δ 192.7, 164.6, 163.2, 159.6, 148.3, 137.6, 133.1, 131.4, 116.6, 115.4, 110.6, 105.7, 82.6, 55.6, 47.5, 36.7, 32.5, 31.3, 26.4, 25.5, 24.6; HRMS (ESI/TOF-Q) m/z calcd for C$_{24}$H$_{33}$NO$_4$Na$^+$ [M + Na]$^+$ 422.2292, found 422.2307.

Synthesis of Substituted Atropisomeric Enone-Imides 1d and 1e. Following a reported procedure,[65] aniline derivative **9** (1.65 mmol, 1 equiv) was placed in a dry round-bottom flask and purged with N$_2$ followed by the addition of dry THF (20 mL). The solution was cooled to −78 °C, and LiHMDS (0.9 equiv) was added dropwise. The solution was stirred at −78 °C for an hour before the slow addition of freshly prepared acid chloride (1.75 mmol, 1.05 equiv). The reaction mixture was allowed to slowly rise to room temperature and stirred for 16 h. After 16 h, the reaction mixture was quenched with H$_2$O, washed with HCl, extracted with ethyl acetate, dried over Na$_2$SO$_4$, concentrated, and purified using column chromatography.

Compound **1d**: colorless solid (65% yield, 2.21 g); mp 90–94 °C; ^{1}H NMR (400 MHz, CHCl$_3$) δ 7.55–7.52 (m, 1H), 7.33–7.29 (m, 1H), 7.23–7.17 (m, 1H), 6.89–6.86 (m, 1H), 6.02 (s, 1H), 5.6 (d, J = 14.9 Hz, 2H), 2.4 (ABq, J = 16.6, 12.1 Hz, 2H), 2.0 (s, 3H), 1.4 (s, 3H), 1.3 (s, 9H); ^{13}C NMR (100 MHz, CDCl$_3$) δ 192.6, 173.0, 167.5, 161.7, 147.8, 142.2, 136.0, 131.2, 129.7, 129.4, 127.4, 124.1, 106.8, 83.8, 47.9, 36.1, 32.0, 27.0, 24.9, 19.4; HRMS (ESI/TOF-Q) m/z calcd for C$_{22}$H$_{27}$NO$_4$Na$^+$ [M + Na]$^+$ 392.1830, found 392.1838.

Compound **1e**: colorless solid (47% yield, 0.837 g); mp 130–132 °C; ^{1}H NMR (400 MHz, CDCl$_3$) δ 7.07–7.06 (m, 1H), 6.83–6.81 (m, 1H), 6.76–6.73 (m, 1H), 6.02 (s, 1H), 5.57 (m, 2H), 3.79 (d, J = 0.6 Hz, 3H), 2.54–2.42 (m, 2H), 2.00 (s, 3H), 1.44 (s, 3H), 1.36 (s, 3H), 1.32 (d, J = 0.6 Hz, 9H); ^{13}C NMR (100 MHz, CDCl$_3$) δ 192.6, 173.2, 167.8, 161.9, 159.8, 149.3, 142.2, 132.2, 128.8, 124.1, 116.0, 111.7, 106.7, 83.8, 55.5, 47.9, 36.1, 31.8, 27.1, 25.0, 19.5; HRMS (ESI/TOF-Q) m/z calcd for C$_{23}$H$_{29}$NO$_5$Na$^+$ [M + Na]$^+$ 422.1925, found 422.1943.

General Irradiation Procedure of Atropisomeric Enones 1a–e with Thioxanone as Photocatalyst/Sensitizer. In a Pyrex test tube, enone **1** (10 mg in 10 mL) and thioxanthone (mol %) were dissolved in a given solvent and then degassed with N$_2$ for 10 min. The solution was irradiated for a specified time interval in a Rayonet reactor (~420 nm). After the reaction, a stock solution of internal standard (triphenylmethane) was added, and this solution was concentrated under reduced pressure to obtain the crude reaction mixture. ^{1}H NMR spectroscopy of the crude reaction mixture was recorded to determine the mass balance and percent yield. For atropselective reactions, optically pure enones were employed.

Direct Irradiation Procedure of Atropisomeric Enones 1. In a Pyrex test tube, enone **1** (10 mg in 10 mL) was dissolved in a given solvent and degassed with N$_2$ for 10 min. The solution was irradiated for the specified time interval in either a Rayonet reactor at ~350 nm/~420 nm or using a 450 W medium-pressure Hg lamp enclosed in a quartz jacket that was cooled with running water. After the reaction, a stock solution of internal standard (triphenylmethane) was added, and this solution was concentrated under reduced pressure to obtain the crude reaction mixture. ^{1}H NMR spectroscopy of the crude reaction mixture was recorded to determine the mass balance and percent yield.

Compound *cis,cis*-**2a**: colorless solid (66% yield, by ^{1}H NMR spectroscopy using internal standard); mp 143–146 °C; ^{1}H NMR (400 MHz, CDCl$_3$) δ 7.50–7.48 (m), 7.27–7.23 (m), 7.02–7.00 (m), 3.87–3.81 (m), 3.49–3.39 (m), 2.88–2.82 (m), 2.46–2.39 (m), 2.25–2.18 (m), 1.97–1.79 (m), 1.39 (s), 1.35 (s), 1.32 (s); ^{13}C NMR (100 MHz, CDCl$_3$) δ 170.9, 147.3, 142.6, 129.7, 128.6, 128.4, 127.9, 80.0, 78.8, 52.1, 51.5, 45.2, 42.8, 42.8, 35.8, 31.8, 30.6, 30.1, 29.9, 24.9.

Crystal data for *cis,cis*-**2a**: C$_{22}$H$_{29}$NO$_3$ (355.46), orthorhombic, *Pccn*, a = 16.2407(5) Å, alpha = 90.00°; b = 18.9857(6) Å, beta = 90.00°; c = 12.4646(4) Å, gamma = 90.00°. *V* = 3843.3(2) Å^3, *Z* = 8, *T* = 100(2) K, absorption coefficient = 0.641 mm^{-1}, reflections collected = 18521, unique = 3387 [*R*(int) = 0.0295], refinement by Full-matrix least-squares on F^2, data/restraints/parameters = 3387/0/240, goodness-of-fit on F^2 = 1.037, final *R* indices [I > 2sigma(I)] R1 = 0.0351, wR2 =

0.0885; *R* indices (all data) R1 = 0.0394, wR2 = 0.0920, largest diff. peak and hole = 0.26 and −0.22 e Å^{-3}, respectively.

Compound *cis,trans*-**2a**: pale yellow solid (22% yield, by ^{1}H NMR spectroscopy using internal standard); ^{1}H NMR (400 MHz, CDCl$_3$) δ 7.54–7.51 (m), 7.28–7.25 (m), 6.94–6.91 (m), 4.22–4.16 (m), 3.40–3.37 (m), 3.34–3.29 (m), 2.82–2.73 (m), 2.59–2.47 (m), 2.36–2.32 (m), 2.30–2.18, 1.96–1.88 (m), 1.45 (s), 1.44 (s), 1.33 (s); ^{13}C NMR (100 MHz, CDCl$_3$) δ 206.5, 171.0, 147.6, 142.5, 130.2, 128.5, 127.8, 127.6, 78.5, 77.8, 77.2, 54.5, 49.6, 45.4, 39.4, 35.8, 31.8, 31.6, 30.5, 30.4, 27.0, 19.7.

Crystal data for *cis,trans*-**2a**: C$_{22}$H$_{29}$NO$_3$ (355.46), monoclinic, C2/c, a = 32.5617(9) Å, alpha = 90.00°; b = 12.2539(3) Å, beta = 98.588(2)°; c = 19.7547(5) Å, gamma = 90.00°. *V* = 7793.9(4) Å^3, *Z* = 16, *T* = 100(2) K, absorption coefficient = 0.33 mm^{-1}, reflections collected = 24883, unique = 6620 [*R*(int) = 0.0436], refinement by Full-matrix least-squares on F^2, data/restraints/parameters = 6620/0/479, goodness-of-fit on F^2 = 1.030, final *R* indices [I > 2sigma(I)] R1 = 0.0472, wR2 = 0.1130; *R* indices (all data) R1 = 0.0601, wR2 = 0.1206, largest diff. peak and hole = 0.55 and −0.32 e Å^{-3}, respectively.

Compound *cis,cis*-**2b**: colorless solid (37% yield, 0.0292 g); ^{1}H NMR (400 MHz, CDCl$_3$) δ 7.57–7.55 (m), 7.33–7.24 (m), 6.99–6.97 (m), 4.49–4.41 (m), 3.88–3.83 (m), 3.19–3.14 (m), 2.55 (s), 2.48–2.42 (m), 2.40–2.33 (m), 2.04–1.85 (m), 1.76–1.64 (m), 1.51–1.48 (m), 1.43 (s), 1.40 (s), 1.32 (s); ^{13}C NMR (100 MHz, CDCl$_3$) δ 210.1, 170.7, 146.8, 141.7, 130.4, 128.7, 127.9, 127.1, 82.5, 78.1, 51.5, 49.4, 42.6, 41.4, 35.9, 31.7, 29.9, 29.1, 27.7, 25.0, 22.9.

Crystal data for *cis-cis*-**2b** (1S,6R, 2R,P)-**2b**: C$_{23}$H$_{31}$NO$_3$ (369.49), orthorhombic, P2(1)2(1)2(1), a = 8.2306(2) Å, alpha = 90.00°; b = 15.6867(5) Å, beta = 90.00°; c = 41.3174(13) Å, gamma = 90.00°. *V* = 4038.3(2) Å^3, *Z* = 8, *T* = 100(2) K, absorption coefficient = 0.629 mm^{-1}, reflections collected = 16255, unique = 6440 [*R*(int) = 0.0199], refinement by Full-matrix least-squares on F^2, data/restraints/parameters = 6440/0/497, goodness-of-fit on F^2 = 1.045, final *R* indices [I > 2sigma(I)] R1 = 0.0265, wR2 = 0.0656; *R* indices (all data) R1 = 0.0276, wR2 = 0.0663, largest diff. peak and hole = 0.14 and −0.18 e Å^{-3}, respectively; Flack parameter = 0.04(5).

Compound *cis,trans*-**2b**: colorless solid (36% yield, 0.0292 g); mp 98–102 °C; C$_{23}$H$_{31}$NO$_3$ (369.49); ^{1}H NMR (400 MHz, CDCl$_3$) δ 7.09–7.08 (m), 6.92–6.90 (m, 1H), 6.79–6.77 (m), 4.47–4.39 (m), 3.88–3.85 (m), 3.83 (s), 3.17–3.12 (m), 2.55 (s), 2.49–2.33 (m), 2.04–1.84 (m), 1.73–1.46 (m), 1.42 (s), 1.40 (s), 1.32 (s); ^{13}C NMR (100 MHz, CDCl$_3$) δ 210.2, 171.0, 158.6, 148.3, 134.8, 131.2, 115.2, 111.0, 82.5, 78.1, 55.3, 51.4, 49.6, 42.6, 41.5, 35.9, 31.6, 29.9, 29.1, 27.7, 25.0, 22.9.

Compound *cis,cis*-**2c**: colorless solid (35% yield, 0.0264 g); mp 139–142 °C; ^{1}H NMR (400 MHz, CDCl$_3$) δ 7.09–7.08 (m), 6.92–6.90 (m, 1H), 6.79–6.77 (m), 4.47–4.39 (m), 3.88–3.85 (m), 3.83 (s), 3.17–3.12 (m), 2.55 (s), 2.49–2.33 (m), 2.04–1.84 (m), 1.73–1.46 (m), 1.42 (s), 1.40 (s), 1.32 (s); ^{13}C NMR (100 MHz, CDCl$_3$) δ 207.1, 174.0, 146.1, 143.7, 130.3, 128.6, 127.8, 127.2, 81.7, 77.6, 53.8, 49.2, 42.2, 41.2, 35.7, 31.7, 30.6, 28.4, 27.2, 26.4, 26.1.

Crystal data for *cis,cis*-**2c**: C$_{24}$H$_{33}$NO$_4$ (399.51), monoclinic, P2(1)/c, a = 20.7554(7) Å, alpha = 90.00°; b = 6.2296(2) Å, beta = 101.719(2)°; c = 17.0708(6) Å, gamma = 90.00°. *V* = 2161.21(13) Å^3, *Z* = 4, *T* = 100(2) K, absorption coefficient = 0.660 mm^{-1}, reflections collected = 21165, unique = 3832 [*R*(int) = 0.0471], refinement by Full-matrix least-squares on F^2, data/restraints/parameters = 3832/0/268, goodness-of-fit on F^2 = 1.050, final *R* indices [I > 2sigma(I)] R1 = 0.0432, wR2 = 0.1058; *R* indices (all data) R1 = 0.0558, wR2 = 0.1135, largest diff. peak and hole = 0.19 and −0.22 e Å^{-3}, respectively.

Compound *cis,trans*-**2c**: colorless solid (35% yield, 0.0264 g); ^{1}H NMR (400 MHz, CDCl$_3$) δ 7.06–7.05 (m, 1H), 6.96–6.94 (m, 1H), 6.77–6.75 (m, 1H), 4.66–4.60 (m, 1H), 3.82 (s, 3H), 3.45–3.40 (t, 1H), 3.12–3.07 (dd, J = 15.2, 5.2 Hz, 1H), 2.75–2.72 (d, J = 15.2 Hz, 1H), 2.51–2.43 (m, 1H), 2.35–2.27 (m, 2H), 2.19–2.03 (m, 2H), 1.84–1.64 (m, 3H), 1.51 (s, 3H), 1.39 (s, 9H), 1.32 (s, 3H); ^{13}C NMR (100 MHz, CDCl$_3$) δ 207.1, 174.2, 158.5, 147.6, 136.9, 131.1, 115.1, 111.1, 81.8, 77.6, 55.3, 54.0, 49.2, 42.3, 41.3, 35.8, 31.5, 30.6, 28.5, 27.2, 26.4, 26.1.

Crystal data for *cis,trans*-**2c**: $C_{24}H_{33}NO_4$ (399.51), triclinic, *P*-1, a = 11.7956(4) Å, alpha = 101.858(2)°; b = 12.4371(4) Å, beta = 99.6140(10)°; c = 16.1837(5) Å, gamma = 105.039(1)°. *V* = 2182.12(12) Å^3, Z = 4, T = 100(2) K, absorption coefficient = 0.654 mm^{-1}, reflections collected = 27433, unique = 7541 [*R*(int) = 0.0238], refinement by Full-matrix least-squares on *F*^{2}, data/restraints/parameters = 7541/0/586, goodness-of-fit on *F*^{2} = 1.045, final *R* indices [*I* > 2sigma(*I*)] *R*1 = 0.0423, w*R*2 = 0.0984; *R* indices (all data) *R*1 = 0.0498, w*R*2 = 0.1033, largest diff. peak and hole = 0.28 and −0.32 e Å^{-3}, respectively.

Compound *cis,cis*-**2d** (mixture of *N*-C$_{Aryl}$ rotamers): colorless solid (67% yield, calculated from ^{1}H NMR spectroscopy); mp 199−201; ^{1}H NMR (400 MHz, CDCl$_3$) δ 7.58−7.56 (m, 1H), 7.40−7.36 (m, 1H), 7.30−7.26 (m, 1H), 6.81−6.78 (m, 1H), 3.17−3.15 (m, 1H), 2.67−2.56 (m, 3H), 2.29−2.24 (m, 1H), 1.47 (s, 3H), 1.42 (s, 3H), 1.39 (s, 3H), 1.28 (s, 9H); ^{13}C NMR (100 MHz, CDCl$_3$; mixture of *N*-C$_{Aryl}$ rotamers) δ 179.2, 176.9, 148.5, 131.5, 130.5, 130.1(d), 130.0, 129.2, 128.6, 127.8, 127.6, 79.4, 79.0, 51.4, 51.3, 47.2, 46.9, 41.1, 40.3, 36.0, 32.0, 31.9, 31.8, 31.4, 31.14, 30.3, 30.2, 29.9, 29.4, 29.2, 15.8, 15.3.

Crystal data for *cis,cis*-**2d** (major rotamer): $C_{22}H_{27}NO_4$ (369.44), monoclinic, *P*2(1)/c, a = 14.8270(14) Å, alpha = 90.00°; b = 10.2711(9) Å, beta = 115.034(4)°; c = 14.4324(13) Å, gamma = 90.00°. *V* = 1991.4(3) Å^3, Z = 4, T = 100(2) K, absorption coefficient = 0.680 mm^{-1}, reflections collected = 8770, unique = 3321 [*R*(int) = 0.0406], refinement by Full-matrix least-squares on *F*^{2}, data/restraints/parameters = 3321/0/250, goodness-of-fit on *F*^{2} = 1.165, final *R* indices [*I* > 2sigma(*I*)] *R*1 = 0.0513, w*R*2 = 0.1591; *R* indices (all data) *R*1 = 0.0671, w*R*2 = 0.1827, largest diff. peak and hole = 0.29 and −0.32 e Å^{-3}, respectively.

Compound *cis,cis*-**2d** (minor *N*-C$_{Aryl}$ rotamer): colorless solid (17% yield, calculated from ^{1}H NMR spectroscopy); mp 201−203 °C; ^{1}H NMR (400 MHz, CDCl$_3$) δ 7.56−7.54 (m, 1H), 7.40−7.35 (m, 1H), 7.28−7.24 (m, 1H), 6.84−6.82 (m, 1H), 3.24−3.20 (m, 1H), 2.79−2.73 (m, 1H), 2.63−2.56 (m, 2H), 2.25−2.20 (m, 1H), 1.46 (s, 3H), 1.44 (s, 3H), 1.40 (s, 3H), 1.31 (s, 9H); ^{13}C NMR (100 MHz, CDCl$_3$) δ 177.1, 147.9, 131.5, 131.0, 131.1, 128.7, 127.8, 78.8, 78.7, 51.4, 46.9, 51.4, 46.9, 40.3, 35.6, 31.5, 31.2, 30.2, 29.2, 15.9.

Crystal data for *cis,cis*-**2d** (minor rotamer): $C_{22}H_{27}NO_4$ (369.44), orthorhombic, P2(1)2(1)2(1), a = 7.9328(3) Å, alpha = 90.00°; b = 14.3352(5) Å, beta = 90.00°; c = 16.9365(7) Å, gamma = 90.00°. *V* = 1925.99(13) Å^3, Z = 4, T = 100(2) K, absorption coefficient = 0.703 mm^{-1}, reflections collected = 12198, unique = 3295 [*R*(int) = 0.0246], refinement by Full-matrix least-squares on *F*^{2}, data/restraints/parameters = 3295/0/251, goodness-of-fit on *F*^{2} = 1.073, final *R* indices [*I* > 2sigma(*I*)] *R*1 = 0.0261, w*R*2 = 0.0660; *R* indices (all data) *R*1 = 0.0266, w*R*2 = 0.0663, largest diff. peak and hole = 0.13 and −0.18 e Å^{-3}, respectively; twin law (−1.0, 0.0, 0.0, 0.0, −1.0, 0.0, 0.0, 0.0, −1.0), BASF [0.40(19)]

Compound *cis,cis*-**2e** (major *N*-C$_{Aryl}$ rotamer): colorless solid (56% yield, 0.112 g); mp 172−185 °C; ^{1}H NMR (400 MHz, CDCl$_3$) δ 7.13−7.12 (m, 1H), 6.85−6.82 (m, 1H), 6.78−7.76 (m, 1H), 3.84 (s, 3H), 3.22−3.17 (m,1H), 2.69−2.63 (m, 3H), 2.29 (dd, *J* = 13.4, 6.7 Hz, 1H), 1.50 (s, 3H), 1.45 (s, 3H), 1.42 (s, 3H), 1.30 (s, 9H); ^{13}C NMR (100 MHz, CDCl$_3$) δ 206.3, 179.4, 176.9, 160.2, 149.8, 130.9, 122.9, 115.5, 111.6, 79.2, 78.8, 55.4, 51.1, 46.9, 40.9, 35.8, 31.8, 31.5, 31.4, 30.1, 29.2.

Crystal data for *cis,cis*-**2e** (major *N*-C$_{Aryl}$ rotamer, $C_{23}H_{29}NO_5$) (1*R*,6*R*,10*R*,*P*)-**2e**: $C_{23}H_{29}NO_5$ (399.47), orthorhombic, P2(1)2(1)-2(1), a = 8.0354(6) Å, alpha = 90.00°; b = 13.7812(10) Å, beta = 90.00°; c = 18.9887(14) Å, gamma = 90.00°. *V* = 2102.8(3) Å^3, Z = 4, *T* = 100(2) K, absorption coefficient = 0.719 mm^{-1}, reflections collected = 12152, unique = 3521 [*R*(int) = 0.0252], refinement by Full-matrix least-squares on *F*^{2}, data/restraints/parameters = 3521/0/269, goodness-of-fit on *F*^{2} = 1.071, final *R* indices [*I* > 2sigma(*I*)] *R*1 = 0.0282, w*R*2 = 0.0708; *R* indices (all data) *R*1 = 0.0287, w*R*2 = 0.0712, largest diff. peak and hole = 0.17 and −0.16 e Å^{-3}, respectively; Flack parameter = 0.06(6).

Photoproduct *cis,cis*-**2e** (minor *N*-C$_{Aryl}$ rotamer): colorless solid (14% yield, 0.028 g); *cis,cis*-**2e** (minor *N*-C$_{Aryl}$ rotamer; $C_{23}H_{29}NO_5$); ^{1}H NMR (400 MHz, CDCl$_3$) δ 7.11−7.10 (m, 1H), 6.84−6.79 (m, 2H), 3.84 (s, 3H), 3.27−3.23 (m, 1H), 2.80 (dd, *J* = 13.6, 10.5 Hz, 1H), 2.73−2.60 (m, 3H), 2.26 (dd, *J* = 13.6, 6.8 Hz, 1H), 1.57 (s, 2H), 1.50 (s, 3H), 1.48 (s, 3H), 1.44 (s, 3H), 1.34 (s, 9H); ^{13}C NMR (100 MHz, CDCl$_3$; minor *N*−C$_{Aryl}$ rotamer) δ 206.2, 179.1, 177.2, 160.2, 149.2, 132.3, 123.3, 115.2, 111.5, 100.0, 78.6, 78.5, 77.2, 55.4, 51.2, 46.6, 40.1, 35.4, 31.2, 31.0, 30.0, 29.1, 15.7.

■ ASSOCIATED CONTENT

Ⓢ Supporting Information

The Supporting Information is available free of charge on the ACS Publications website at DOI: 10.1021/acs.joc.6b01066.

Experimental procedures, structure of compounds **10**−**17**, XRD analysis, characterization data, and analysis conditions (PDF)
Single crystal XRD (CIF)

■ AUTHOR INFORMATION

Corresponding Author
*E-mail: jayaraman.sivaguru@ndsu.edu.

Notes

The authors declare no competing financial interest.

■ ACKNOWLEDGMENTS

■ REFERENCES

(1) Turro, N. J.; Schuster, G. *Science* **1975**, *187*, 303.
(2) Oppolzer, W. *Acc. Chem. Res.* **1982**, *15*, 135.
(3) Namyslo, J. C.; Kaufmann, D. E. *Chem. Rev.* **2003**, *103*, 1485.
(4) Iriondo-Alberdi, J.; Greaney, M. F. *Eur. J. Org. Chem.* **2007**, *2007*, 4801.
(5) Dembitsky, V. M. *J. Nat. Med.* **2007**, *62*, 1.
(6) Bach, T.; Hehn, J. P. *Angew. Chem., Int. Ed.* **2011**, *50*, 1000.
(7) Wrobleski, M. L.; Reichard, G. A.; Paliwal, S.; Shah, S.; Tsui, H.-C.; Duffy, R. A.; Lachowicz, J. E.; Morgan, C. A.; Varty, G. B.; Shih, N.-Y. *Bioorg. Med. Chem. Lett.* **2006**, *16*, 3859.
(8) Bauslaugh, P. G. *Synthesis* **1970**, *1970*, 287.
(9) Tateyama, S.; Masuo, S.; Suvannasara, P.; Oka, Y.; Miyazato, A.; Yasaki, K.; Teerawatananond, T.; Muangsin, N.; Zhou, S.; Kawasaki, Y.; Zhu, L.; Zhou, Z.; Takaya, N.; Kaneko, T. *Macromolecules* **2016**, *49*, 3336.
(10) Li, Y.; Urbas, A.; Li, Q. *J. Org. Chem.* **2011**, *76*, 7148.
(11) Li, Y.; Wang, M.; Wang, H.; Urbas, A.; Li, Q. *Chem. - Eur. J.* **2014**, *20*, 16286.
(12) Sun, R.; Xue, C.; Ma, X.; Gao, M.; Tian, H.; Li, Q. *J. Am. Chem. Soc.* **2013**, *135*, 5990.
(13) Ramamurthy, V. In *Photochemistry in Organized and Constrained Media*; Ramamurthy, V., Ed.; Wiley-VCH: New York, 1991; p 429.
(14) Vallavoju, N.; Sivaguru, J. *Chem. Soc. Rev.* **2014**, *43*, 4084.
(15) Pemberton, B. C.; Raghunathan, R.; Volla, S.; Sivaguru, J. *Chem. - Eur. J.* **2012**, *18*, 12178.
(16) Kranz, D. P.; Griesbeck, A. G.; Alle, R.; Perez-Ruiz, R.; Neudörfl, J. M.; Meerholz, K.; Schmalz, H.-G. *Angew. Chem., Int. Ed.* **2012**, *51*, 6000.
(17) Bergonzini, G.; Schindler, C. S.; Wallentin, C.-J.; Jacobsen, E. N.; Stephenson, C. R. J. *Chem. Sci.* **2014**, *5*, 112.
(18) Condie, A. G.; González-Gómez, J. C.; Stephenson, C. R. J. *J. Am. Chem. Soc.* **2010**, *132*, 1464.
(19) Nagib, D. A.; MacMillan, D. W. C. *Nature* **2011**, *480*, 224.
(20) Narayanam, J. M. R.; Stephenson, C. R. J. *Chem. Soc. Rev.* **2011**, *40*, 102.

(21) Nicewicz, D. A.; MacMillan, D. W. C. *Science* **2008**, *322*, 77.

(22) Arceo, E.; Montroni, E.; Melchiorre, P. *Angew. Chem. Int. Ed.* **2014**, *53*, 12064.

(23) Tucker, J. W.; Zhang, Y.; Jamison, T. F.; Stephenson, C. R. J. *Angew. Chem., Int. Ed.* **2012**, *51*, 4144.

(24) Curran, D. P.; DeMello, N. C. *J. Chem. Soc., Chem. Commun.* **1993**, 1314.

(25) Curran, D. P.; Qi, H.; Geib, S. J.; DeMello, N. C. *J. Am. Chem. Soc.* **1994**, *116*, 3131.

(26) Thayumanavan, S.; Beak, P.; Curran, D. P. *Tetrahedron Lett.* **1996**, *37*, 2899.

(27) Curran, D. P.; Geib, S.; DeMello, N. *Tetrahedron* **1999**, *55*, 5681.

(28) Clayden, J. *Angew. Chem., Int. Ed. Engl.* **1997**, *36*, 949.

(29) Clayden, J. *Synlett* **1998**, *1998*, 810.

(30) Clayden, J. In *Organic Synthesis Highlights IV*; Wiley-VCH Verlag GmbH, 2000; p 48.

(31) Clayden, J. *Chem. Commun.* **2004**, 127.

(32) Clayden, J.; Lai, L. W.; Helliwell, M. *Tetrahedron* **2004**, *60*, 4399.

(33) Kumarasamy, E.; Raghunathan, R.; Sibi, M. P.; Sivaguru, J. *Chem. Rev.* **2015**, *115*, 11239.

(34) Ayitou, A. J.-L.; Sivaguru, J. *J. Am. Chem. Soc.* **2009**, *131*, 5036.

(35) Ayitou, A. J.-L.; Vallavoju, N.; Ugrinov, A.; Sivaguru, J. *Photochem. Photobiol. Sci.* **2011**, *2011*, 1380.

(36) Ayitou, A. J.-L.; Sivaguru, J. *Chem. Commun.* **2011**, *47*, 2568.

(37) Ayitou, A. J.-L.; Clay, A.; Kumarasamy, E.; Jockusch, S.; Sivaguru, J. *Photochem. Photobiol. Sci.* **2014**, *13*, 141.

(38) Ayitou, A. J.-L.; Jesuraj, J. L.; Barooah, N.; Ugrinov, A.; Sivaguru, J. *J. Am. Chem. Soc.* **2009**, *131*, 11314.

(39) Jesuraj, J. L.; Sivaguru, J. *Chem. Commun.* **2010**, *46*, 4791.

(40) Kumarasamy, E.; Jesuraj, J. L.; Omlid, J. N.; Ugrinov, A.; Sivaguru, J. *J. Am. Chem. Soc.* **2011**, *133*, 17106.

(41) Raghunathan, R.; Kumarasamy, E.; Iyer, A.; Ugrinov, A.; Sivaguru, J. *Chem. Commun.* **2013**, *49*, 8713.

(42) Kumarasamy, E.; Sivaguru, J. *Chem. Commun.* **2013**, *49*, 4346.

(43) Iyer, A.; Jockusch, S.; Sivaguru, J. *J. Phys. Chem. A* **2014**, *43*, 1816.

(44) Kumarasamy, E.; Raghunathan, R.; Jockusch, S.; Ugrinov, A.; Sivaguru, J. *J. Am. Chem. Soc.* **2014**, *136*, 8729.

(45) Kärkäs, M. D.; Porco, J. A.; Stephenson, C. R. J. *Chem. Rev.* **2016**, ASAP DOI: 10.1021/acs.chemrev.5b00760.

(46) Crimmins, M. T. *Chem. Rev.* **1988**, *88*, 1453.

(47) Turro, N. J.; Ramamurthy, V.; Scaiano, J. C. *Modern Molecular Photochemistry of Organic Molecules*; University Science Books: Sausalito, CA, 2010.

(48) Schuster, D. I.; Lem, G.; Kaprinidis, N. A. *Chem. Rev.* **1993**, *93*, 3.

(49) De Mayo, P. *Acc. Chem. Res.* **1971**, *4*, 41.

(50) Fort, D. A.; Woltering, T. J.; Nettekoven, M.; Knust, H.; Bach, T. *Angew. Chem., Int. Ed.* **2012**, *51*, 10169.

(51) Sylvie Le, B.; Jean-Pierre, P.; Olivier, P. *Tetrahedron Lett.* **1993**, *34*, 635.

(52) Refer to Supporting Information.

(53) Wolf, C. *Dynamic Stereochemistry of Chiral Compounds. Principles and Applications*; RSC Publishing: Cambridge, UK, 2008.

(54) Trapp, O. Springer: Berlin Heidelberg, 2013; p 1.

(55) Betson, M. S.; Clayden, J.; Helliwell, M.; Johnson, P.; Lai, L. W.; Pink, J. H.; Stimson, C. C.; Vassiliou, N.; Westlund, N.; Yasin, S. A.; Youssef, L. H. *Org. Biomol. Chem.* **2006**, *4*, 424.

(56) Clayden, J.; Lai, L. W. *Tetrahedron Lett.* **2001**, *42*, 3163.

(57) Only *cis,cis*-**2b** was investigated for enantioselectivity due to limitations in separating enantiomers of *cis,trans*-**2b** on a chiral stationary phase.

(58) Satzger, H.; Schmidt, B.; Root, C.; Zinth, W.; Fierz, B.; Krieger, F.; Kiefhaber, T.; Gilch, P. *J. Phys. Chem. A* **2004**, *108*, 10072.

(59) Meyer, C.; Piva, O.; Pete, J.-P. *Tetrahedron* **2000**, *56*, 4479.

(60) Vallavoju, N.; Selvakumar, S.; Jockusch, S.; Sibi, M. P.; Sivaguru, J. *Angew. Chem., Int. Ed.* **2014**, *53*, 5604.

(61) Vallavoju, N.; Selvakumar, S.; Jockusch, S.; Prabhakaran, M. T.; Sibi, M. P.; Sivaguru, J. *Adv. Synth. Catal.* **2014**, *356*, 2763.

(62) Vallavoju, N.; Selvakumar, S.; Pemberton, B. C.; Jockusch, S.; Sibi, M. P.; Sivaguru, J. *Angew. Chem., Int. Ed.* **2016**, *55*, 5446.

(63) Neumann, J. J.; Rakshit, S.; Dröge, T.; Glorius, F. *Angew. Chem., Int. Ed.* **2009**, *48*, 6892.

(64) Brecker, L.; Pogorevc, M.; Griengl, H.; Steiner, W.; Kappe, T.; Ribbons, D. W. *New J. Chem.* **1999**, *23*, 437.

(65) Amougay, A.; Pete, J.-P.; Piva, O. *Tetrahedron Lett.* **1992**, *33*, 7347.